

A Comparative Study on Aluminium Pillared Smectite Synthesis from Synthetic Saponite and Indonesian Montmorillonite

Is Fatimah^a

Shaobin Wang^b

Karna Wijaya^c

Narsito^c

^a*Chemistry Department, Islamic University of Indonesia, Yogyakarta, Indonesia*

^b*Chemical Engineering Department, Curtin University of Technology, Perth, WA 6845, Australia*

^c*Chemistry Department, Gadjah Mada University, Sekip Utara Bls 21, Bulak Sumur, Yogyakarta, Indonesia*

E-mail : isfatimah@fmipa.uui.ac.id

Synthesis of aluminium pillared smectite from two raw clays, saponite and Indonesian montmorillonite, has been investigated. The clays were characterized by XRD, N₂ adsorption isotherm, DTA-TGA, surface acidity measurements using pyridine-FTIR method, and evaluated for catalytic esterification reaction. The characterization indicated an increase in d_{001} by metal oxide pillar, increase in BET specific surface area, and surface acidity. DTA-curves showed exothermic peaks in the range of 100-130°C and 400-800°C. TGA curves showed an increase in thermal stability of pillared clays. For both kinds of clays, it was also observed that pillarization reduced weight loss at high temperature. Esterification reaction rate constant and surface acidity data showed that the Brønsted acidity dominantly affects the reaction mechanism compared with the effect of specific surface area and Lewis acid site. Montmorillonite and pillared montmorillonite exhibited higher catalytic activity than saponite and pillared saponite although the specific surface areas of the latter are higher.

Keywords: pillarization, smectite, XRD, esterification

INTRODUCTION

Acid catalysts are extensively employed in chemical and petrochemical industries. They are claimed to be responsible for producing various products of more than

10⁸ ton/year. However, environmentally friendly catalysts are needed for green chemistry. Homogeneous acid catalysts are generally toxic to environment and it is difficult to recycle them. Thus heterogeneous catalysts are currently widely used. For this purpose,

organic transformations using inorganic solid acid catalyst are gaining more attention due to simple separation of product, mild reaction conditions, high selectivity, ease in recovery and reuse of the catalysts, as well as reduction in the generation of wasteful byproducts. High specific surface area, crystallinity and chemical stability are important characters needed for heterogeneous catalysts (Lazlo 1990, Eng-Poh et al., 2007)

Clays have been used as acidic catalysts in petroleum cracking and several other organic reactions. For stable performance, interest is now focused on pillared clays (PILCs), which possess larger two-dimensional pores allowing big molecules to react and both Brønsted and Lewis acidity can be accessed. In previous investigations, a class of clay, smectite, was mainly used including montmorillonite and saponite minerals. Several metal oxides have been reported as pillars, such as Al, Zr, Ti, Cr, and mixed metal such as Ga-La, Cr-Al in order to gain designed character of materials. Among these metals, the intercalation of clays with polyoxocations of Al^{3+} is mostly investigated. The main pillaring agent is $[AlO_4Al_{12}(OH)_x^{24+}(H_2O)_{12-x}]^{(7-x)+}$ (briefly Al_{13}). Its capability to exchange native cation in silica sheet of smectite and to form aluminium oxide pillar in calcination step are the main reasons for wide use (Kloprogge 1998, Ding et al. 2001).

However, the characters of Al-PILCs are significantly influenced by synthesis parameters and physicochemical properties of raw clays (Gil et al. 2000, Vicente et al. 2004). In the present work, synthesis of aluminium pillared saponite and montmorillonite was reported. The study is focused on a comparison of the physicochemical properties of PILCs during aluminium pillarization using two different clays. Several analytical techniques have been employed including XRD, BET surface area analysis, surface acidity measurement (pyridine adsorption followed by FTIR spectroscopy), and DTA-TGA. The catalyst

activity in ethyl acetate esterification was further evaluated. These complementary techniques will allow us to understand the significant changes in properties resulted from pillarization process, specially specific surface area, thermal stability, acid distribution and strength as well as the acid centers for acid catalyzed reaction.

EXPERIMENTAL METHODS

The starting clays were synthetic saponite supplied by Kunimine Industry Co. Japan, and natural montmorillonite provided by PT. Tunas Inti Makmur, Semarang, Indonesia. The cation exchange capacities of the two clays are 99 and 68 meq/100 g for saponite and montmorillonite, respectively. Particle sizes of less than 200 mesh were used in pillaring process.

Synthesis of Aluminium Pillared Clays

A typical synthesis procedure of aluminium pillared clay was as follows: $AlCl_3 \cdot 6H_2O$ solution was slowly titrated with NaOH solution to obtain pillar solution with OH/Al molar ratio of 2.0. The resulted solution was aged overnight under stirring at room temperature. The pillaring solution was then slowly added to a suspension of saponite or montmorillonite in deionized water at a concentration of 5% (w/v). The mixture was stirred and allowed to react. Finally, the solid was filtrated and washed with deionized water until it was chloride free (tested by $AgNO_3$ solution). The solid obtained was dried in an oven for 24 h and calcined at the temperature of 400 °C for 4 h. The solid sample was designated as PILS for aluminium pillared saponite or PILM for aluminium-pillared montmorillonite.

Characterization

Elemental analyses of SiO_2 and Al_2O_3 in both clays were performed by a gravimetric method, and other elements, Na, Ca and Mg,

were analyzed by Atomic Absorption Spectrophotometry. The solids were also characterized by X-ray diffraction using a Shimadzu XRD X6000 diffractometer with Cu K α radiation and Ni filter. BET surface area analyzer NOVA 1000 was used for determining specific surface area of materials. Thermal transformation and stability were studied by DTA-TGA analysis. The scanning was operated at a temperature range of 30-800°C and heating rate of 3 °C/min.

Surface acidity was determined by two methods: gravimetric analysis of ammonia adsorption to identify total surface acidity and FTIR analysis of adsorbed pyridine by using a FTIR Nicolet Avatar spectrometer to identify Brønsted-Lewis acid sites. Solids were put in vacuum at 130°C for 5 h before adsorbed pyridine vapor in desiccator. Adsorption was conducted overnight. FTIR spectroscopy analysis was performed after degassed for 1 h at the pressure of 0.3 atm.

The catalytic activity of pillared saponites and montmorillonite were evaluated in an esterification reaction. The esterification of acetic acid was carried out with ethanol in a three necked 100 ml flask equipped with a thermometer and a magnetic stirrer. The temperature was maintained at reflux temperature at certain variation time of reaction. The products of the reaction were filtered by Whatman 41 filter paper and formation of ester was monitored using a Gas Chromatography analyzer (Shimadzu GC QP 5000).

RESULT AND DISCUSSION

Elemental analysis results of two raw clays are presented in Table 1. It is shown that the content of MgO dominates in saponite, while in contrast, SiO₂ and Al₂O₃ are the major chemical components in montmorillonite. Saponite consists of tetrahedrally silica and octahedrally alumina in the ratio of 2:1 and in

the analogous structure, octahedral sheet in montmorillonite consists of alumina. In the interlayer spaces there are some exchangeable cations giving cation exchange capacity (CEC). It is measured that the CEC of saponite is higher than that of montmorillonite. According to the values of sodium and calcium contents, both smectite samples are sodium smectite due to higher content of sodium than calcium. It is suggested that the swelling properties can accommodate intercalation process.

The XRD patterns of aluminium pillared smectites are presented in Fig 1. The reflections at $2\theta = 6.10^\circ$ ($d = 14.47 \text{ \AA}$) and $2\theta = 19.89^\circ$ ($d = 4.46 \text{ \AA}$) in montmorillonite sample are correspondence to d_{001} and d_{004} of montmorillonite structure and the analogous reflections are shown at 6.59° ($d=13.34\text{\AA}$) and at $2\theta= 19.88^\circ$ ($d=4.46 \text{ \AA}$). Reflection at $2\theta = 21.71^\circ$ ($d = 4.09 \text{ \AA}$) appearing in the XRD pattern of montmorillonite is evidence for silica (SiO₂) as impurities. After the pillarization, the basal spacing d_{001} is shifted to the left, corresponding to the increase in d_{001} . The d_{001} basal spacing for saponite and aluminium pillared saponite is 13.34 and 15.56 \AA , while the corresponding basal spacing for montmorillonites and aluminium pillared montmorillonite is 14.47 and 19.47 \AA , respectively, as shown in Table 2. Clearly the intercalation was successful as expected. Estimating the silicate layer thickness shows 9.5 \AA , the gallery height for aluminium pillared montmorillonite is slightly larger ($19.47-14.47= 5.00 \text{ \AA}$) than that of aluminium pillared saponite ($15.79 -13.34 = 2.45 \text{ \AA}$).

The results of surface area also show the pore evolution after pillarization. The specific surface areas of the materials are listed in Table 2.

The d_{001} values and the BET specific surfaces of the pillared materials are increased compared with those of the raw montmorillonite and saponite samples. Both effects are also confirmed by the increase in

micropore as shown by higher micropore volume of pillared materials than that of parent

Table 1. Elemental analysis result of montmorillonite and saponite

Mineral/element	Content (%)	
	Saponite	Montmorillonite
SiO ₂	13.54	29.14
Al ₂ O ₃	5.10	17.74
MgO	46.75	5.38
Ca	0.05	0.58
Na	7.66	5.25
Cation Exchange capacity (meq/100gram)	89.90- 99.90	68.00-69.72

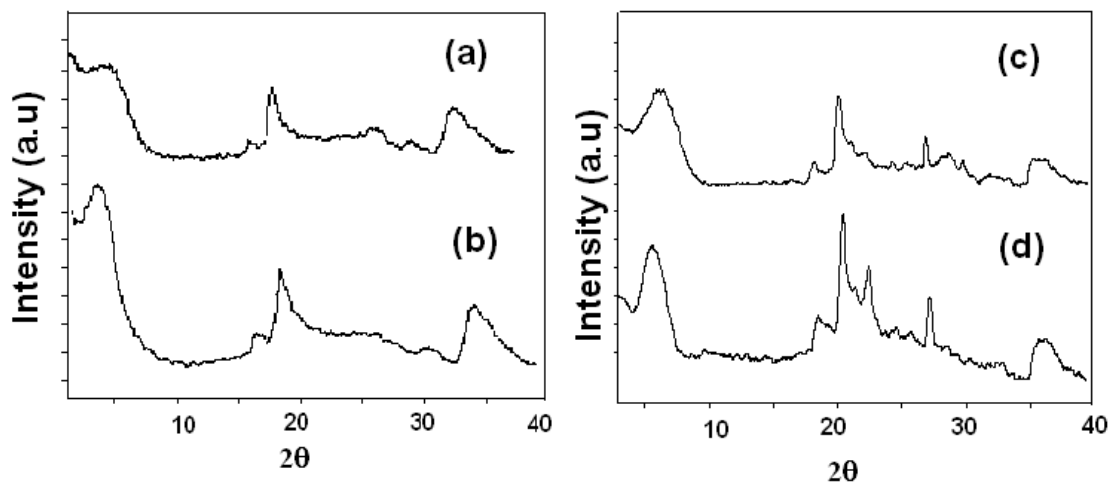


Fig 1. XRD pattern of (a) saponite (b) Al-PILS (c) montmorillonite (d) Al-PILM

Table 2. Specific surface area and basal spacing of materials

Sample	Specific surface area (m ² /g)	Basal spacing d ₀₀₁ (nm)	V _{micropore} (cc/g)
Montmorillonite	45.90	14.47	9.87.10 ⁻³
PILM	183.09	19.47	14.40.10 ⁻³
Saponite	166.47	13.34	19.01.10 ⁻³
PILS	261.49	15.79	30.53.10 ⁻³

materials. Table 3 shows the results of surface acidity measurement by using n-butylamine titration and ammonia adsorption method. The principle of n-butylamine titration is acid-base reaction to protonic acid (H⁺) monitored by potentiometer. Equivalent point in the

titration shows the amount of Brønsted acid center in samples. On the other hand, NH₃ adsorption on the surface represents total acidity of the surface on which both Brønsted and Lewis acid sites will chemically adsorb NH₃. Data in Table 3 present the strong correlation

of surface acidity after pillarization. In general, pillarization generates more acidity on the smectite samples.

Table 3. Surface acidity of materials

Sample	Brønsted acidity (meq/g)	NH ₃ adsorbed (meq/g)
Montmorillonite	0.092	0.309
PILM	0.103	0.360
Saponite	0.064	0.303
PILS	0.087	0.343

From specific surface area and pore volume data, it can be inferred that porous structure in montmorillonite exhibits more ionic species in surface as produced by isomorphous substitution in structure.

By comparing both acid species, it can be inferred that the increasing of Brønsted acid after pillarization are not proportional to the increasing of NH₃ adsorbed on surface. Montmorillonite and saponite samples show that the increasing of NH₃ adsorbed is slightly higher than the increasing of the Brønsted acidity. These data may be correlated with specific surface area of the materials. From Table 2, it is seen that montmorillonite and saponite pillarization significantly increase the specific surface area of materials. Porous structure of pillared materials arise new sites for NH₃ adsorption. Lewis acidity are strongly correlated with this type of sites, which generally arises from exposed Al at the edges and dominates when the interlayer water is largely removed. Brønsted acidity arises from the protons formed by the dissociation of interlayer water due to the polarizing effect of multivalent cations present in interlayer space (Tyagi et al., 2006). To confirm the presence of both acid sites, FTIR analysis after pyridine adsorption was investigated. The spectra are presented in Fig. 2.

The evidence of the Lewis acid site can be shown at the spectra region of 1400-1700 cm⁻¹. The FTIR spectra of adsorbed pyridine in

all samples will show the presence of intense bands around 1636, 1550, 1500 and 1450 cm⁻¹ which correspond to pyridine interaction with clay surface. The band at around 1636 cm⁻¹ is detected for all samples, related to pyridine adsorbed on the Brønsted acid sites. The other band localized at 1545-1555 cm⁻¹ is assigned to pyridine adsorbed on Brønsted acid sites and the band at 1445-1455 cm⁻¹ is attributed to pyridine adsorbed on Lewis acid sites as reported by Carvalho et al.(2000) and Ahenach et al. (2000).

The spectra of raw clays and pillared clays show the similar FT-IR pattern. In saponite, spectrum at 1441.98 cm⁻¹ shifted to 1448.01 cm⁻¹ in pillared saponite are the evidence of Lewis acid sites. The Brønsted acidity sites are indicated by the spectra at 1636.11 cm⁻¹ and 1635.98 cm⁻¹ for saponite and pillared saponite, respectively. Analogous spectra were recorded for montmorillonite and pillared montmorillonite, but there are two different peaks observed at 998.02 cm⁻¹ and 525.07 cm⁻¹. Both of spectra indicated silica and metal oxide in samples.

Furthermore, the effect of pillarization on the thermal stability was studied by DTA-TGA and the curves are depicted in Figure 3. TGA plots of saponite and montmorillonite showed a loss of 15.4 wt.% and 11.6 wt % below 130 °C, respectively, due to dehydration (loss of physically adsorbed water). Water loss in this temperature range is an indication for non crystalline hydrated water. It is seen that the water adsorbed on saponite is higher than that on montmorillonite, probably due to higher specific surface area and pore volume of saponite.

For both types of clays, pillared samples have less weight loss in this region compared to the raw clays. Rigid form produced by pillarization makes the pillared samples not as swellable as raw forms. In agreement with the weight loss in this region, weight loss at the region of 130-200°C and 450-

800°C also show the similar effect. Between 130

and 200°C a very small weight loss (0.4 wt.%)

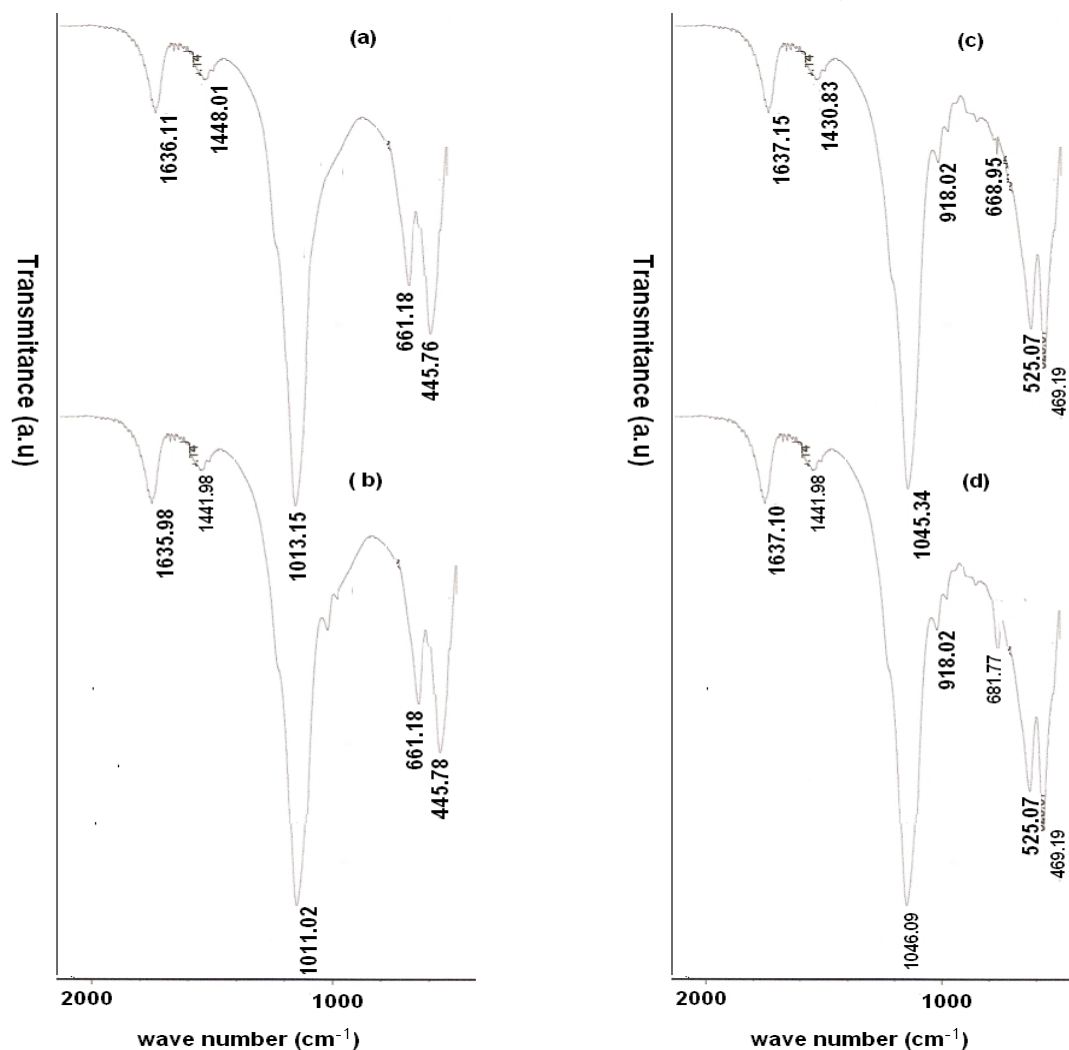


Fig 2. FTIR spectra after pyridine adsorption. (a) saponite (b) pillared saponite (c) montmorillonite (d) pillared montmorillonite

was observed in pillared montmorillonite and 4% was observed in pillared saponite. These weight losses are lower than those on raw saponite (5%) and montmorillonite (1.6%). These weight losses are attributed to the removal of interlayer water and the onset of dehydroxylation (Kloprogge et al., 1994). The dehydroxylation of the clay structure and its subsequent collapse caused a maximum weight loss of 4.0 wt.% between 450 and 800°C in pillared saponite and 5% in saponite. In the same way, the heating caused 2% weight loss in montmorillonite and 1% in pillared montmorillonite. DTA curves of all materials show a similar pattern. An exothermic peak at

the region of 100-120°C represents the loss of physisorbed water. Other exothermic and endothermic peaks at the range of 400-800°C is possibly caused by thermal transformation in high temperature.

In general, we can conclude that montmorillonite and pillared montmorillonite are more thermally stable than saponite and pillared saponite. Effect of impurities in samples is the main factor in this case. However, DTA profiles of montmorillonite and pillared montmorillonite show the exothermic peak in the region of 400-800°C that are attributed to metal oxide pillar deformation during the heating. For saponite and pillared

saponite samples, same reason is also applied. It has been known that the stability of the

pillars is related to the dehydroxylation process

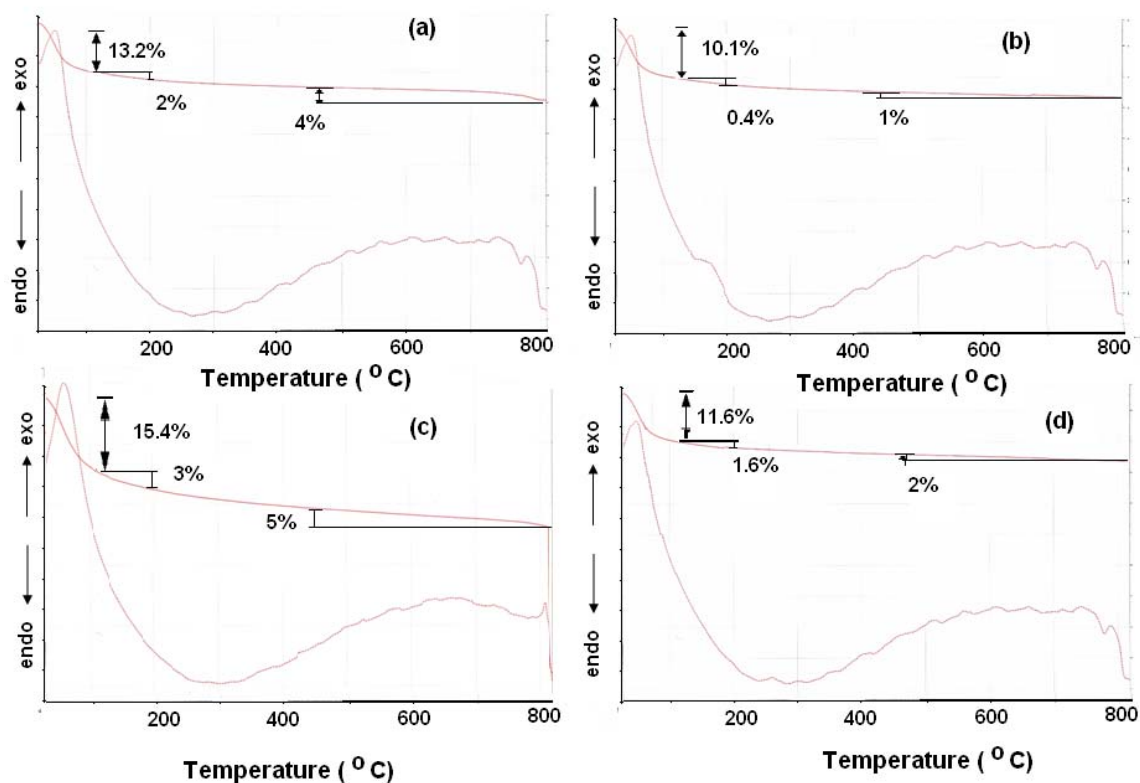


Fig 3. TGA-DTA curve of (a) Al-PILS (b) Al-PILM (c) Saponite (d) Montmorillonite

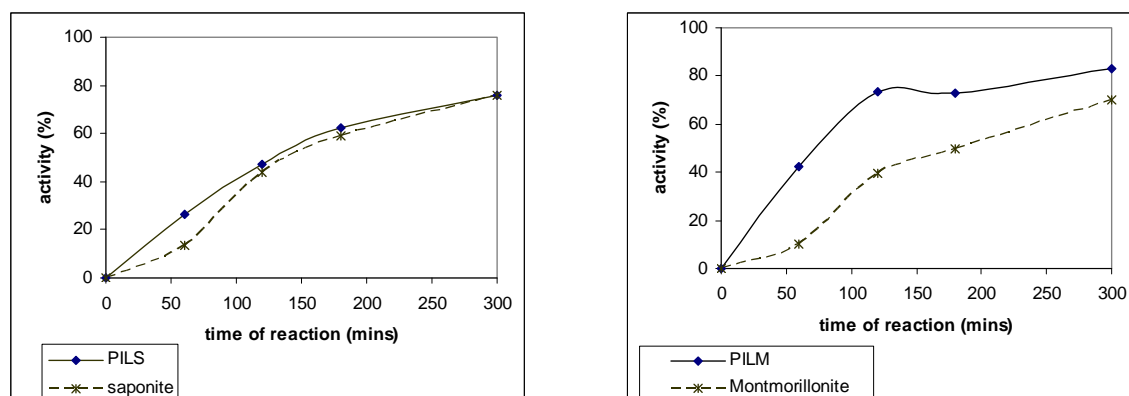


Fig 4. Catalytic activity as a function of time over catalysts (a) Montmorillonite and Pillared Montmorillonite (b) Saponite and Pillared Saponite

that negatively affects the basal spacing (Molina et al., 2000).

Catalyst Activity

In order to study the effect of changes in physicochemical characters, acid catalyzed reaction with ethyl acetate synthesis was

conducted. For all samples, the reaction condition was maintained constant, the reaction temperature is 90°C and catalyst mass (mg) to total volume (mL) is 1:20. Fig. 4 shows the variation of catalytic activity as a function of reaction time.

Reaction conversions were measured as the concentration of ethyl acetate in products that were analyzed by a gas chromatography. The reaction of esterification is second order, depending on each reactant.

$$V = -\frac{\partial[\text{ethanol}]}{\partial t} = -\frac{\partial[\text{acetic acid}]}{\partial t} = +\frac{\partial[\text{ethyl acetate}]}{\partial t} = k[\text{ethanol}][\text{acetic acid}] \quad (1)$$

$$\frac{1}{[\text{ethanol}]_0 - [\text{acetic acid}]_0} \log \frac{[\text{ethanol}]_t}{[\text{acetic acid}]_t} = \frac{1}{[\text{ethanol}]_0 - [\text{acetic acid}]_0} \log \frac{[\text{ethanol}]_0}{[\text{acetic acid}]_0} + kt \quad (2)$$

The rate constant k is determined by plotting logarithmic values of ethanol to acetic acid ratio against the time of reactions, in which k is the slope of the curve. The values of k for different catalysts were determined and are listed in Table 4.

Table 4. Rate Constant of Catalyzed Reaction

Catalyst	k (L/M.min)
Saponite	0.5434×10^{-3}
PILS	1.371×10^{-3}
Montmorillonite	0.636×10^{-3}
PILM	2.577×10^{-3}

CONCLUSIONS

Pillarization of saponite and montmorillonite with aluminium pillar produced better materials with higher specific surface area, basal spacing d_{001} and thermal stability. More importantly, pillared clays present much surface Lewis and Bronsted acidity, which results in the increase of catalytic activity upon esterification reaction of ethanol and acetic acid. Studies on the kinetics of the reaction suggest the domination of Bronsted acidity in the esterification mechanism over the Lewis acidity.

REFERENCE

Ahenach, J., Cool, P., Vansant, E.F.(2000). "Enhanced Brønsted Acidity Created Upon Al-grafting of Porous Clay

Thus the rate constant equation is expressed in the following equations:

Heterostructures **via** Aluminium Acetylacetonate Adsorption". *Phys. Chem. Chem. Phys.*, **2**, pp. 5750-5755.

Carvalho, A., Martins, A., Silva, J., Pires, J., Vasques, P., Carvalho, B.(2000). "Acidity Characterization Of Al- And Zr-Pillared Clays". *Clays and Clay Minerals*, **51** (3), pp. 340-349.

Ding, Z., Klopogge, J.T., Frost, R.L.(2001). "Porous Clays and Pillared Clays-Based Catalysts. Part 2: A Review of the Catalytic and Molecular Sieve Applications". *Journal of Porous Materials*, **8**, pp.273-293.

Eng-Poh Ng, Nur, H., Wong, K., Muhid, M., Hamdan, H.(2007). "Generation of Brønsted acidity in AlMCM-41 by sulphation for enhanced liquid phase tert-butylation of phenol". *Applied Catalysis A: General*, **323**, pp. 58-65.

Gil, A., Vicente, A., Gandia, M.(2000). "Main Factor Controlling the Texture of Zirconia and Alumina Pillared Clay". *Microporous and Mesoporous materials*, **34**, 115-125.

Klopogge, J.T.(1998) "Synthesis of Smectites and Porous Pillared Clay Catalysts: A Review". *Journal of Porous Materials*, **5**, pp. 5-41.

Lazlo, P. (1990). "Catalysis of organic reactions by inorganic solids". *Pure & Appl. Chem.*, **62**(10), pp. 2027-2030.

Molina, R., Moreno, G., Poncelet (2000). "Al-pillared hectorite and montmorillonite prepared from concentrated clay suspensions: structural, textural and catalytic properties". *Studies in Surface Science and Catalysis*, **130**(2), pp. 983-988.

Tyagi, B., Chudasama, C.D., Jasra, R.V. (2006). "Characterization of surface acidity of an acid montmorillonite activated with hydrothermal, ultrasonic and microwave techniques." *Applied Clay Science*, **31**, pp. 16–28.

Vicente, M.A., Belver, C., Trujillano, R., Rives, V., Álvarez, A.C., Lambert, J.-F., Korili, G. and Gil, A. (2004). "Preparation and characterisation of Mn- and Co-supported catalysts derived from Al-pillared clays and Mn- and Co-complexes". *Applied Catalysis A: General*, **267**, pp. 47–58.